J. Neurovirol. (2011) 17:570–577
DOI 10.1007/s13365-011-0066-x

Investigation of varicella-zoster virus neurotropism and neurovirulence using SCID mouse–human DRG xenografts

Leigh Zerboni · Ann Arvin

Received: 29 September 2011 / Revised: 11 November 2011 / Accepted: 20 November 2011 / Published online: 8 December 2011

Abstract Varicella-zoster virus (VZV) is a medically important human alphaherpesvirus. Investigating pathogenic mechanisms that contribute to VZV neurovirulence are made difficult by a marked host restriction. Our approach to investigating VZV neurotropism and neurovirulence has been to develop a mouse–human xenograft model in which human dorsal root ganglia (DRG) are maintained in severe compromised immunodeficient (SCID) mice. In this review, we will describe our key findings using this model in which we have demonstrated that VZV infection of SCID DRG xenograft results in rapid and efficient spread, enabled by satellite cell infection and polykaryon formation, which facilitates robust viral replication and release of infectious virus. In neurons that persist following this acute replicative phase, VZV genomes are present at low frequency with limited gene transcription and no protein synthesis, a state that resembles VZV latency in the natural human host. VZV glycoprotein I and interaction between glycoprotein I and glycoprotein E are critical for neurovirulence. Our work demonstrates that the DRG model can reveal characteristics about VZV replication and long-term persistence of latent VZV genomes in human neuronal tissues, in vivo, in an experimental system that may contribute to our knowledge of VZV neuropathogenesis.

L. Zerboni (✉) · A. Arvin
Department of Pediatrics,
Stanford University School of Medicine,
300 Pasteur Dr.,
Stanford, CA 94305, USA
e-mail: zerboni@stanford.edu

A. Arvin
Department of Microbiology and Immunology,
Stanford University School of Medicine,
Stanford, CA 94305, USA

Keywords Varicella-zoster virus · Neuropathogenesis · Neurotropism · Glycoprotein E · Glycoprotein I · SCID

Varicella-zoster virus (VZV) is a member of the Alphaherpesvirinae and the etiological agent of the ubiquitous childhood viral infection commonly known as "chickenpox". While VZ virions share many physical and biochemical properties that distinguish herpesviruses, VZV possesses unique pathogenic features that are not shared by the other human neurotropic alphaherpesviruses, herpes simplex virus type 1 and type 2 (HSV) (Cohen et al. 2007).

Primary VZV infection is initiated upon inhalation of respiratory droplets containing infectious particles (Arvin et al. 2010). Robust replication facilitates infection of susceptible T lymphocytes in mucosa-associated lymphoid tissues. VZV-infected T-lymphocytes with skin homing phenotypes infiltrate and infect dermal sites leading to development of the characteristic pruritic rash on the skin surface within 10–21 days (Ku et al. 2002, 2004). The capacity to infect and replicate within T-lymphocytes, which is not shared by HSV, enables two different mechanisms for VZV neurotropism. Sensory nerve ganglia may acquire virus via retrograde axonal transport in neurons innervating cutaneous and mucosal sites of replication or through circulating T cells that enter neuronal ganglia and transfer virus to sensory neurons. Similar to HSV, VZV persists within the infected host as a lifelong latent infection in sensory nerve ganglia from which it may reactivate, resulting in anterograde transport of infectious particles that re-infect dermal sites causing a painful rash known as herpes zoster. Whereas HSV is associated with many reactivation events over the lifetime of the infected individual, VZV reactivation is usually limited to a single event (Cohen et al. 2007). The capacity to cause significant neuropathic pain following an

episode of herpes zoster (post-herpetic neuralgia) is another clinical feature that distinguishes VZV from HSV. Differences in the route of neuronal infection and in the frequency and severity of reactivation suggest that VZV and HSV may have evolved different strategies for neurovirulence in the human host.

The pathogenic mechanisms through which VZV causes neurovirulence are difficult to investigate because, unlike HSV, VZV replicates poorly across a species barrier. Human cadaveric tissues from individuals who died during primary varicella infection or reactivation are rare. Examination of latently infected cadaver ganglia cannot provide information concerning early events in VZV neuronal infection. Our approach to investigating VZV neurotropism and neurovirulence has been to develop a mouse–human xenograft model in which human dorsal root ganglia (DRG) are maintained in severe compromised immunodeficient (SCID) mice (Zerboni et al. 2010). Xenotransplanted DRG maintains an organotypic microenvironment so that VZV infection of human neurons can be examined under "in vivo" conditions. In this brief review, we will describe the SCID DRG model and discuss our key findings using this model with respect to initial events in VZV replication, spread, satellite glial cell tropism, polykaryon formation between neurons and encapsulating satellite cells, latency, and the molecular requirements for VZV glycoprotein E (gE) and glycoprotein I (gI).

Methods for implantation and VZV infection of DRG xenografts in SCID mice

DRG xenograft implantation Our procedures for implantation of human dorsal root ganglia into immunodeficient SCID mice have been previously described, but we will review them briefly (Zerboni et al. 2005, 2007). All of our animal protocols and procedures have been reviewed and approved by the Stanford University Administrative Panel on Laboratory Animal Care. Human tissues are procured by Advanced Bioscience Resources (Alameda, CA) in accordance with state and federal regulations. Tissues are used within 24 h after extraction. Individual dorsal root ganglions, including a portion of the dorsal root, are dissected from fetal spinal tissues and kept on ice until transplanted. A single ganglion (1.5–2 mm^3) is loaded into a 16-gauge lubricated transplantation needle. Six-week-old male *scid/scid* homozygous C.B.17 mice are anesthetized, and a small incision is made along the abdominal wall to expose the left kidney. The kidney capsule is perforated, and the DRG is inserted under the renal capsule. After the transplantation needle is withdrawn, the DRG can be easily seen through the kidney capsule. The abdominal wall and skin incision are closed, and mice are given a post-surgical analgesic and monitored on a warming pad until awakening.

At 4 weeks after transplantation, DRG xenografts can be assessed for viability and engraftment. An incision is made in the abdominal wall to expose the xenograft. At that time, the graft can be macroscopically analyzed for indicators of good engraftment and viability such as pink shiny color and neovascularization, indicating anastomosis to the host vasculature (Fig. 1a, arrow denotes implanted DRG). Nonviable xenografts have a dull pale appearance. In general, good engraftment occurs in >95% of surgeries.

Histological evaluation of DRG xenografts Histological evaluation of DRG xenografts at 4 weeks after transplantation reveals an architecture that resembles normal human DRG, with abundant neuronal cell bodies encapsulated by satellite glial cells, within a network of axons and fibroblasts (Fig. 1b) (Zerboni et al. 2005). Endothelial cells within the microvasculature express the human-specific cell marker PECAM-1 (Zerboni et al. 2005). In the developing human, peripheral sensory neurons arise from three waves of neural crest cell (NCC) migration to DRG (Marmigere and Ernfors 2007; Montelius et al. 2007). Fetal tissues are used at 18–21 gestational weeks, by which time major events in sensory neurogenesis (NCC migration and DRG condensation) have occurred (Marmigere and Ernfors 2007; Montelius et al. 2007). The major subdivisions of DRG neuronal populations, large-diameter RT97+ neurons and small-diameter TrkA+ nociceptors, are present in DRG xenografts. DRG neurons express human-specific neuronal cell markers with the expected subcellular localization patterns such as neural cell adhesion molecule (NCAM), which is distributed along the cell surfaces of neurons and satellite cells, herpes viral entry mediator (HVEM/HveA), and synaptophysin, a major synaptic vesicle protein. DRG xenografts can be maintained in SCID mice for an extended period of time (>5 months).

VZV infection of DRG xenografts At 4 weeks after transplantation, DRG xenografts are ready for infection experiments (Zerboni et al. 2005). DRG xenografts are inoculated by direct injection of VZV-infected fibroblasts using a 30-gauge needle. The needle is inserted through the kidney capsule, and a small volume (10 μl, ~1,000 PFU, $\sim 3 \times 10^4$ cells) is slowly injected into the DRG xenograft. The needle is held in place for 15 s to prevent leakage from the needle track. The incision is closed, and mice are monitored until they awaken.

At specific timepoints after infection, mice are euthanized and the DRG xenograft is removed for analysis. Methods for assessment of VZV-infected DRG xenografts have been described in detail (Oliver et al. 2008; Reichelt et al. 2008; Zerboni et al. 2005, 2007, 2010, 2011a). For histological assessment, DRG are immersion fixed in 4% paraformaldehyde and paraffin-embedded (Zerboni et al. 2005). Serial sections (10 μm) are made through the entire implant, and

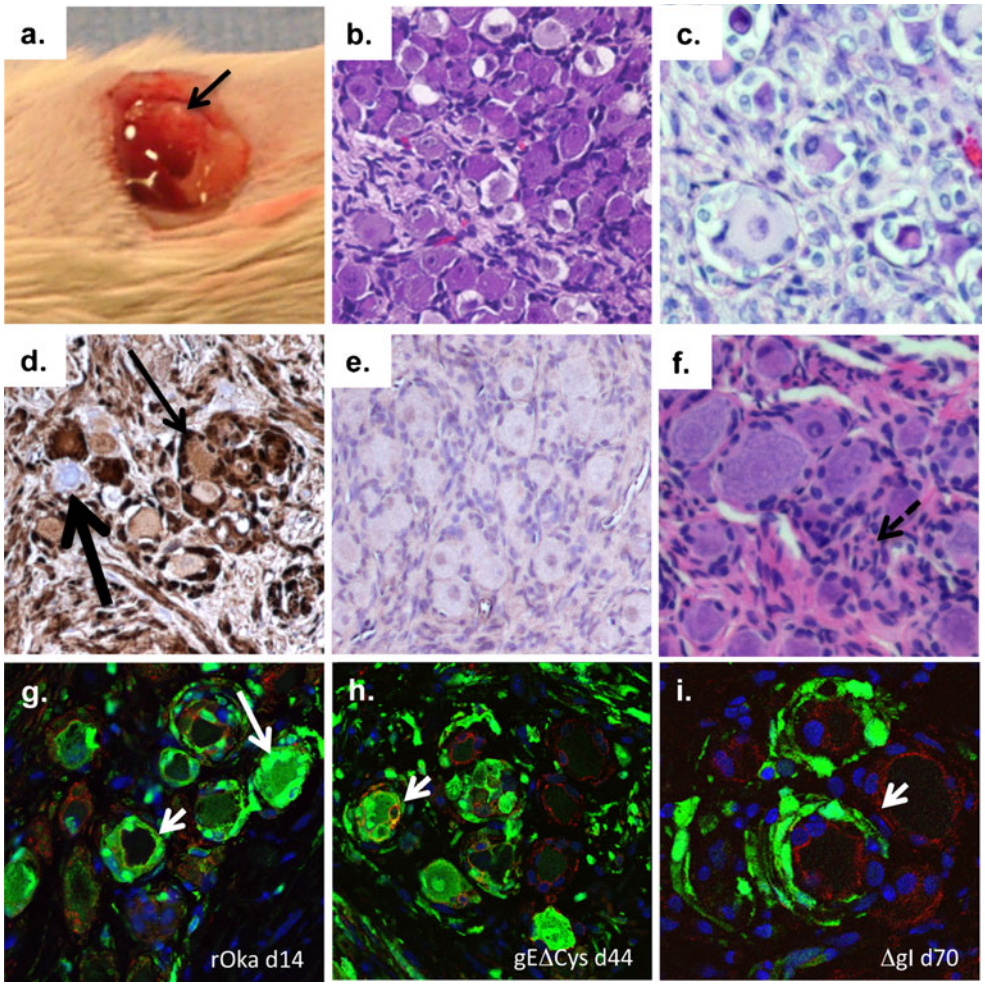

Fig. 1 **a** DRG xenograft in SCID mouse 4 weeks after xenotransplantation. **b** Hematoxylin and eosin (H&E)-stained tissue section of uninfected SCID DRG xenograft. **c** H&E-stained tissue section; VZV-infected SCID DRG xenograft 14 days after infection with neurons exhibiting cytopathic effect. **d** DAB (*brown*)-immunohistochemistry of VZV-infected SCID DRG xenograft 14 days after infection using a rabbit polyclonal antibody to IE63. The majority of neurons express VZV proteins at this time point (*thin arrow*), but some neurons are observed that do not express VZV proteins (*thick arrow*). **e** DAB (*brown*)-immunohistochemistry of VZV-infected SCID DRG xenograft 56 days after infection using a rabbit polyclonal antibody to IE63, counterstained with hematoxylin. No IE63-positive neurons are observed. **f** H&E-stained tissue section 56 days after infection; microsatellite cell proliferations indicate neuronal cell loss (*dashed arrow*), but many neurons persist following resolution of VZV infection. **g**–**i** Confocal immunofluorescent staining of DRG infected with rOka at day 14 (**g**), rOka gEΔCys at day 44 (**h**), and rOkaΔgI at day 70 (**i**). Sections are stained with antibody to neural cell adhesion molecule (Alexa-594, *red*), anti-IE63 (Alexa-488, *green*), and counterstained with Hoechst. The *short arrows* in (**g**–**i**) indicate neurons with intact NCAM staining of neuronal membranes, which indicates lack of polykaryon formation. The *long arrow* in (**g**) indicates polykaryon formation in rOka-infected tissue sections, which occurs in up to 50% of neuron–satellite cell complexes. Some panels in this composite image were adapted from panels that appeared in previous publications (see references): Zerboni et al. 2005, 2007, 2011a

every 20th section is stained with hematoxylin and eosin to identify regions of interest for further analysis by immunostaining or in situ hybridization. Quantitative DNA/RNA real-time polymerase chain reaction (PCR) is performed using the 5′-exonuclease method. For imaging experiments, bioluminescence is measured at 3–5-day intervals following intraperitoneal injection with D-luciferin. Mice are imaged using an IVIS Spectra imaging system (Xenogen), and bioluminescence (photons per meter per second squared) is calculated using Living Image Software (Caliper Life Sciences).

VZV infection of DRG xenografts

Acute VZV replication in DRG xenografts We have used VZV–luciferase reporter viruses to sequentially assess viral replication within the DRG xenograft in living animals. In the experiment shown in Fig. 2a, b and c, DRG xenografts were infected with a recombinant VZV that expresses firefly luciferase driven by the immediate early regulatory gene ORF62 promoter, as a marker for lytic replication (Jones et al. 2006). As expected for a human restricted virus, the bioluminescent signal was restricted to the region of the

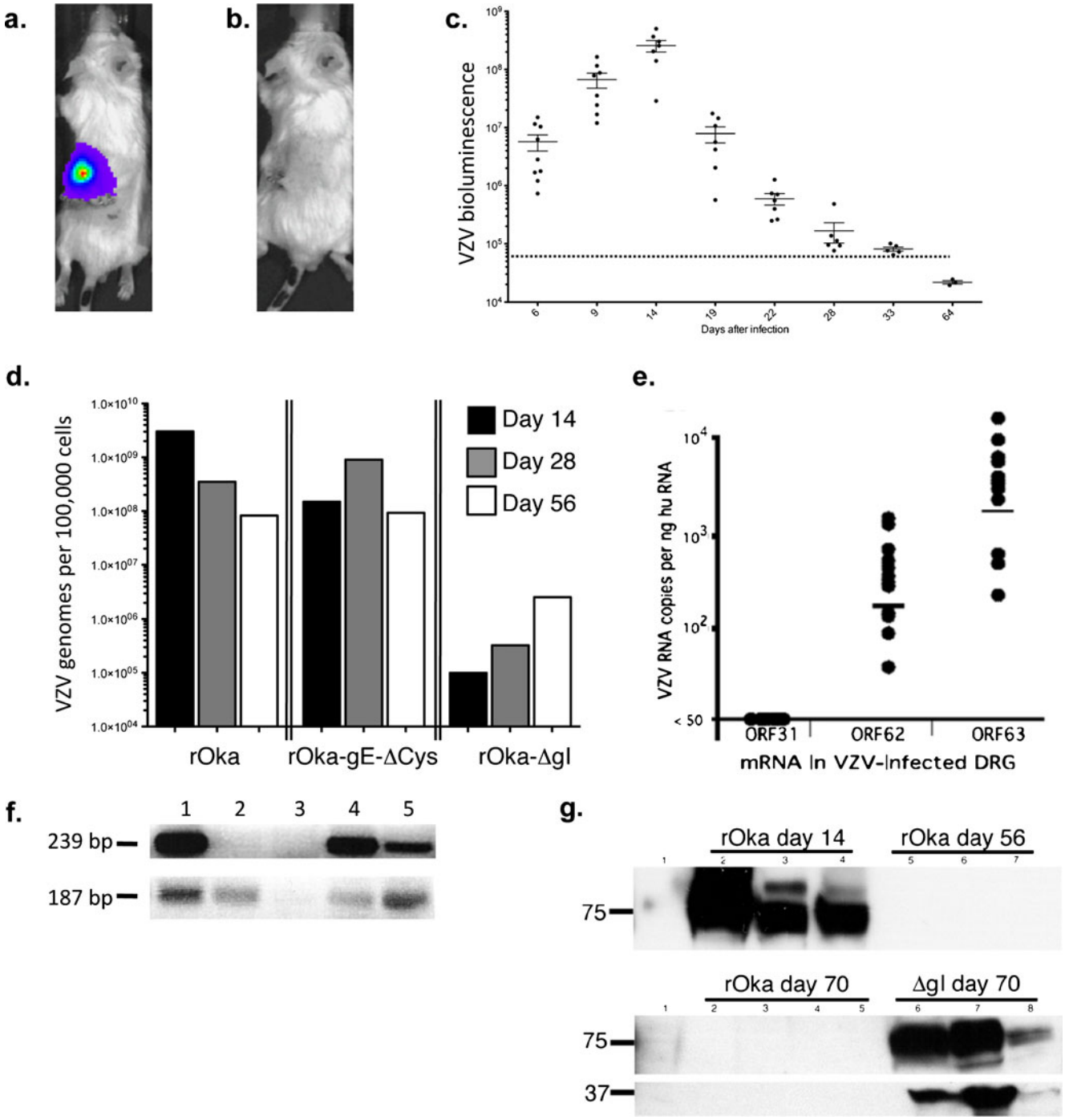

Fig. 2 **a**–**c** The kinetics of VZV DRG infection can be monitored using VZV-expressing luciferase. **a** SCID DRG mouse infected with VZV–luciferase at 14 days after infection; the bioluminescent signal is restricted to the region of the left kidney. **b** SCID DRG mouse infected with VZV contains a promoterless luciferase cassette. **c** Course of VZV DRG infection using VZV expressing luciferase under control of the IE62 promoter. The *dotted line* indicates average bioluminescence in the promoterless control virus. **d** VZV genome copies in rOka, rOka gEΔCys, and ΔgI viruses at 14, 28, and 56 days after infection. **e** Quantitative real-time PCR for VZV mRNAs corresponding to ORFs 31 (gB), 62, and 63 at 56 days after infection. *Circles* represent individual DRG. **f** Standard PCR of DNA extracted from SCID xenografts using primers to amplify a 239-bp fragment of VZV ORF9a (*top*) and a 187-bp fragment of cellular β-globin (*bottom*). *Lane 1*, VZV-infected SCID mouse skin xenograft (day 21 post-infection); *lane 2*, uninfected skin xenograft; *lane 3*, human fetal DRG (prior to implantation); *lane 4*, VZV-infected DRG at day 14 after infection and day 56 (*lane 5*) after infection. **g** Immunoblot of DRG extracts using (*top blot*) human polyclonal anti-VZV antibody; *lane 1*: uninfected DRG, *lanes 2–4*: rOka-infected DRG, day 14; *lanes 5–7*: rOka-infected DRG, day 56. Immunoblot of DRG extracts (*bottom two blots*) using human polyclonal anti-VZV antibody (*top*) or rabbit polyclonal anti-IE63 IgG (*bottom*); *lane 1*: uninfected DRG; *lanes 2–5*: rOka-infected DRG, day 70; *lanes 6–8*: rOkaΔgI-infected DRG, day 70. Some panels in this composite image were adapted from panels that appeared in previous publications (see references): Zerboni et al. 2005, 2007, 2011a

DRG xenograft (Fig. 2a). As a negative control, SCID DRG mice were infected in parallel with a virus containing a promoterless firefly luciferase cassette; no signal was detected (Fig. 2b). As shown in Fig. 2c, bioluminescent values rose rapidly in the first 14 days following VZV–luciferase inoculation and then slowly declined reaching levels equivalent to measurements in mice infected with non-luciferase-expressing VZV by day 33. Live animal imaging using a recombinant VZV that expresses firefly luciferase as a fusion with the immediate early protein 63 (IE63) demonstrated a similar pattern (Oliver et al. 2008).

In a separate set of experiments, we demonstrated recovery of infectious virus from homogenized VZV-infected DRG at 14 days after infection (~70% of DRG), only rarely at day 28 (~12%), but not at day 56 and beyond (0%) (Zerboni et al. 2005, 2007). Taken together, these data indicate that the first 14-day interval following VZV ganglionic infection is characterized by a robust replicative phase within the infected ganglion that resolves, i.e., no infectious virus production, within 8 weeks post-inoculation.

VZV cytopathic effect, satellite cell infection, and polykaryon formation in DRG xenografts Histological analysis of VZV-infected DRG at 14 days after infection reveals that most neurons express VZV proteins (Fig. 1d, thin arrow). However, neurons are observed that do not express VZV proteins (Fig. 1d, thick arrow). Within neurons that express VZV proteins, significant cytopathic changes are observed (Fig. 1c) (Zerboni et al. 2005). Evaluation of acutely infected DRG by ultrathin sections examined by electron microscopy (EM) revealed that satellite cells as well as neurons participate in virion production (Reichelt et al. 2008). Cytoplasmic and intranuclear viral capsids were observed within satellite cells surrounding some infected neurons (Reichelt et al. 2008). In a portion (~50%) of those VZV-infected neuron–satellite cell complexes, neuronal cell membranes had reorganized and fused with the membranes of the encapsulating satellite cells, forming multinuclear structures that resemble polykaryons that are characteristic of VZV skin infection (Reichelt et al. 2008). By confocal immunofluorescence, using the neuronal cell marker NCAM, examples of satellite cell nuclei with no apparent membrane separating them from the neuronal cell body are readily observed (Fig. 1g) (Zerboni et al. 2011a). The capacity for satellite cell infection and polykaryon formation may enhance VZV spread by providing a mechanism to amplify infectious virus progeny; however, in that satellite glial cells are critical regulators of neuronal homeostasis, disruption of the boundaries between neurons and satellite cells is likely to result in neuronal cell death. The consequences of VZV satellite cell infection and polykaryon formation may explain the increased severity of the herpes zoster rash compared with HSV reactivation. These virulence features may also contribute to neuropathic consequences of VZV reactivation, such as post-herpetic neuralgia.

Characteristics of VZV latency in DRG xenografts As shown in Fig. 1d, at the peak of VZV replication (14 days after infection), neurons are observed that do not express VZV proteins, suggesting that some neurons resist VZV replication. Histological analysis of VZV-infected DRG at 56 days after infection reveals that neurons are still maintained in DRG xenografts (Fig. 1e). At the tissue level, satellite cell microproliferations indicate regions of neuronal cell loss (Fig. 1f, dashed arrow). However, clusters of neurons persist that express neural-specific cell markers (not shown) and do not express VZV proteins (Fig. 1e). The persistence of neurons in DRG xenografts several weeks after VZV DRG inoculation, in the absence of infectious virus production, suggests that VZV ganglionic infection may be intrinsically self-limiting. The resolution of lytic replication within the DRG xenograft occurs without any requirement for adaptive immune responses, which SCID mice lack.

Detection of VZV DNA by PCR (Fig. 1f) and quantitative real-time PCR (Fig. 1d) within DRG neurons that persist following lytic replication indicates that those neurons that were not permissive for lytic infection harbor latent genomes. At 14 days after VZV DRG infection, VZV genome copies are typically detected in the range of 10^8–10^{10} copies per 100,000 cells; by day 56, VZV genome copy numbers are significantly reduced but are consistently detected above background values in uninfected DRG, at 10^6–10^8 copies per 100,000 cells (Fig. 2d) (Zerboni et al. 2005, 2007, 2011a). In latently infected human cadaver ganglia, VZV DNA persists in 1.0–6.9% of neurons, and VZV genome copies have been widely estimated at 9–6,000 copies per 100,000 cells (Pevenstein et al. 1999; Wang et al. 2005). Our estimates in neurons that persist in DRG after cessation of VZV replication are higher, but this is expected as autopsied human cadaver ganglia are usually examined many decades after primary VZV infection.

Unlike HSV, VZV latency is not characterized by transcription of a region associated with latency, i.e., latency-associated transcripts (Cohen et al. 2007). In analyses of the VZV transcriptome in cadaver ganglia from individuals who died without evidence of herpes zoster, transcripts corresponding to VZV genes of all kinetic classes have been detected; RNAs corresponding to ORFs 63, 62, 21, and 29 are the most consistently reported (Cohrs et al. 1996, 2000; Nagel et al. 2011). The consistent detection of ORF63 mRNA suggests that IE63 transcription may be a characteristic of VZV latency (Cohrs et al. 2000). In an analysis of the presence of VZV mRNA in SCID DRG xenografts at day 56 after infection, transcripts corresponding to IE63

were most abundant with some IE62 transcripts, but no mRNA corresponding to the late viral glycoprotein gB were detected (Fig. 2e) (Zerboni et al. 2005). These quantitative real-time RNA PCR data demonstrate that, similar to observations in latently infected human cadaver ganglia, VZV genomes that persist in SCID DRG xenografts exhibit limited viral gene transcription.

Our experiments using the SCID DRG xenograft model indicate that VZV protein synthesis is not a characteristic of VZV latency in human neurons. In VZV-infected SCID DRG xenografts at 56 days after infection, VZV proteins are not detected by immunostaining (Fig. 1e), or when DRG cell lysates are examined by immunoblot (Fig. 2g) (Zerboni et al. 2007). Analyses of VZV protein synthesis during neuronal latency in human cadaver ganglia have been discordant, and all have relied exclusively on immunostaining methods. Several studies have reported abundant expression of IE63 and other "latency-associated proteins", such as IE62 and proteins corresponding to ORFs 4, 21, 29, and 66 (Grinfeld and Kennedy 2004; Hufner et al. 2006; Lungu et al. 1998; Theil et al. 2003; Cohrs et al. 1996); whereas others (Mahalingam et al. 1996; Kennedy et al. 1998, 1999) have described IE63 protein expression in cadaver DRG as rare.

We conducted an extensive examination of cadaver ganglia and determined that IE63 protein expression in latently infected sensory neurons is an extremely rare occurrence (Zerboni et al. 2011a). In those rare IE63-positive neurons, co-expression of VZV glycoprotein E suggests an abortive or subclinical reactivation event, rather than bona fide latency (Zerboni et al. 2011a). In further support of only rare expression of VZV proteins during latency, we recently identified an immunostaining artifact that occurs in sensory neurons from individuals with blood type A (Zerboni et al. 2011b). This staining artifact may explain apparent positive staining attributed to VZV rabbit antisera and some ascites-derived anti-VZV monoclonal antibodies that contain endogenous anti-A antibodies (Zerboni et al. 2011b).

Summary of results using intact recombinant VZV Our investigations using intact recombinant VZV and VZV–luciferase reporter viruses have demonstrated that initial events in VZV infection of SCID DRG xenografts are characterized by efficient spread in neurons, enabled by satellite cell infection and polykaryon formation, resulting in robust viral replication and release of infectious virus. In neurons that persist following this acute replicative phase, VZV genomes are present at low frequency with limited gene transcription and no protein synthesis, in a state that resembles latency in the natural human host. In the next part of this review, we will discuss our progress defining determinants of VZV neurovirulence using recombinant viruses with targeted mutations in VZV glycoprotein E and gI.

Contributions of VZV gE and gI to neurovirulence

VZV gE and gI are type I membrane proteins encoded by open reading frames 68 and 67, respectively. Both VZV gE and gI share features with orthologous herpesviral species, such as the formation of gE/gI heterodimers that participate in cell–cell spread (Cohen et al. 2007). HSV and pseudorabies virus (PRV) gE and gI proteins have been shown to participate in anterograde axonal transport and neuron-to-neuron spread in neuronal cultures and small animal models (Ch'ng and Enquist 2005; Dingwell et al. 1995; Polcicova et al. 2005; Saldanha et al. 2000). The cytoplasmic domain of PRV gI also contributes to neurovirulence in a manner that is independent of gE/gI interaction (Card et al. 1992; Tirabassi and Enquist 2000). We examined the capacity for recombinant Oka viruses containing deletions or mutations in gE and gI, or in gI promoter regulatory domains, to replicate in SCID DRG xenografts (Zerboni et al. 2007, 2011a). Acute replication and persistence in a latent state were assessed by quantitative real-time DNA PCR, infectious virus release assay, and evaluation of tissue sections for cytopathic effect, satellite cell tropism, and polykaryon formation (Zerboni et al. 2007, 2011a).

VZV glycoprotein E A portion of the VZV gE N-terminal ectodomain is not conserved in other alphaherpesviruses, and this portion contains regions that are critical for replication in skin and T cell (thy/liv) xenografts in SCID mice (Berarducci et al. 2006, Berarducci et al. 2010). We examined the requirement for a portion of this region (amino acids 27–90) for VZV neuronal infection. The recombinant virus gEΔ27-90 lacks amino acids 27–90, and this abolishes gE interaction with insulin-degrading enzyme, a putative VZV entry receptor (Berarducci et al. 2010; Li et al. 2006, 2007). Although gEΔ27-90 exhibited decreased cell–cell spread in skin xenografts, it was not impaired in DRG xenografts (Berarducci et al. 2010; Zerboni et al. 2011a). Compared with recombinant Oka, the gEΔ27-90 mutant had equivalent VZV genome copies at day 14 and day 56, infectious virus release was similar, and there were no significant differences in spread, satellite cell infection, or polykaryon formation. Mutation of two endodomain motifs, the AYRV motif that mediates gE trafficking to the trans-*Golgi* network and a SSTT acidic cluster motif, had little or no effect on DRG infection or persistence (Moffat et al. 2004; Zerboni et al. 2011a; Zhu et al. 1996).

Mutation of the cysteine-rich region in the VZV gE ectodomain that abolishes interaction between VZV gE and gI had a significant effect on DRG infection (Zerboni et al. 2011a). The gEΔCys mutant was significantly impaired at early times after infection as demonstrated by reduced cytopathic effect and spread, indicating that gE/gI interaction is critical for efficient neuron–neuron

transmission in DRG (Zerboni et al. 2011a). Unlike the expected pattern of decreasing VZV genome copies over time, VZV genomes increased between days 14 and 28 after infection (Fig. 2d). As shown in Fig. 1h, IE63 protein (green) was prominently expressed at 44 days after infection, which was equivalent to rOka-infected DRG at day 14. Dingwell and colleagues noted a similar requirement for HSV gE/gI interaction for spread within synaptically linked neurons (Dingwell et al. 1994, 1995).

Although the capacity to infect satellite cells was intact, the distribution of NCAM on neuronal cell surfaces demonstrated that the gEΔCys mutant had a reduced capacity for polykaryon formation compared with intact rOka (Fig. 1h, short arrow). Deficiencies in cytopathic effect, neuron–neuron transmission, and polykaryon formation would be expected to enhance neuronal survival; however, as infection progressed, we observed a marked fibrosis and microsatellite cell proliferations that indicate areas of neuronal cell loss. By day 56, large areas of gEΔCys-infected DRG xenografts contained acellular fields. These unexpected pathological changes suggest that mislocalization of gE that occurs in the absence of gE/gI interaction may have toxic effects in ganglionic cells. Alternatively, the slow spread of the gEΔCys mutant in DRG xenografts may have overstimulated cellular pathways that mediate the fibrotic response to neuronal damage.

VZV glycoprotein I Mutation of gI promoter elements through which cellular transcription factors Sp1 and USF bind had no effect on DRG infection, although replication of both rOka-gI-Sp1 and rOka-gI-Sp1/USF was diminished in skin and T cell xenografts (Ito et al. 2003; Zerboni et al. 2007). Complete deletion of gI had a dramatic effect on spread of VZV within DRG xenografts. Rather than the typical short replicative phase characterized by high VZV genome copies and infectious virus production that slowly transitions to long-term persistence by day 56 (i.e., latency), infection with the recombinant virus rOkaΔgI resulted in an extremely prolonged replicative phase with slowly increasing VZV genomes over an 8-week interval (Fig. 2d) (Zerboni et al. 2007). While not strictly required for replication, histopathic effect at day 70 was minimal with very few cells exhibiting cytopathology, although infectious virus was recovered from minced tissues and VZV proteins were detected by immunoblot (Fig. 2e). In histological sections, uninfected neurons were observed surrounded by VZV-infected satellite cells (Fig. 1i), which suggests that gI may be a critical component of VZV entry into sensory neurons. Similar to the gEΔCys mutant, the normal membrane localization of gE was impaired, and instead gE was only detected within a few foci within the neuronal cytoplasm (Zerboni et al. 2007). However, we did not observe the severe pathological changes that characterized infection with the gEΔCys mutant. Instead, unusual Golgi stacks and disorganized rough ER containing gE were observed by immuno-EM staining of ultrathin sections (Zerboni et al. 2007). Polykaryon formation was more severely effected than with the gEΔCys mutant. Taken together, these results indicate that VZV entry into sensory neurons may require gI and the capacity for polykaryon formation is a pathogenic mechanism that greatly facilitates neuron–neuron spread in DRG xenografts.

Conclusion

Many questions about VZV neuropathogenesis remain unanswered, in particular, concerning the state of VZV during neuronal latency. We have made progress in defining pathogenic features and molecular requirements for VZV neuronal infection that contribute to clinical manifestations of varicella and herpes zoster. We hope that further investigation using the SCID DRG xenograft model will contribute to our understanding of VZV molecular virology and pathogenesis that may inform and improve future approaches to treatment and prevention of VZV-related disease.

Acknowledgments We thank past and present members of the Arvin lab, many of whom contributed to these experiments, especially Mike Reichelt, Stefan Oliver, Xibing Che, Jaya Rajamani, Preeti Sikka, and Michelle Lai. We also thank Dr. Raymond A. Sobel, Professor of Pathology, Stanford University School of Medicine, for helpful discussions and collaborations. This work was supported by grants AI20459 and AI053846 from the National Institute of Allergy and Infectious Diseases and grant CA049605 from the National Cancer Institute.

References

Arvin AM, Moffat JF, Sommer M, Oliver S, Che X, Vleck S, Zerboni L, Ku CC (2010) Varicella-zoster virus T cell tropism and the pathogenesis of skin infection. Curr Top Microbiol Immunol 342:189–209

Berarducci B, Ikoma M, Stamatis S, Sommer M, Grose C, Arvin AM (2006) Essential functions of the unique N-terminal region of the varicella-zoster virus glycoprotein E ectodomain in viral replication and in the pathogenesis of skin infection. J Virol 80:9481–9496

Berarducci B, Rajamani J, Zerboni L, Che X, Sommer M, Arvin AM (2010) Functions of the unique N-terminal region of glycoprotein E in the pathogenesis of varicella-zoster virus infection. Proc Natl Acad Sci USA 107:282–287

Card JP, Whealy ME, Robbins AK, Enquist LW (1992) Pseudorabies virus envelope glycoprotein gI influences both neurotropism and virulence during infection of the rat visual system. J Virol 66:3032–3041

Ch'ng TH, Enquist LW (2005) Efficient axonal localization of alphaherpesvirus structural proteins in cultured sympathetic neurons requires viral glycoprotein E. J Virol 79:8835–8846

Cohen J, Straus S, Arvin A (2007) Varicella-zoster virus replication, pathogenesis, and management. In: Knipe D, Howley P (eds) Fields virology. Lippincott-Williams & Wilkins, Philadelphia, pp 2774–2818

Cohrs RJ, Barbour M, Gilden DH (1996) Varicella-zoster virus (VZV) transcription during latency in human ganglia: detection of transcripts mapping to genes 21, 29, 62, and 63 in a cDNA library enriched for VZV RNA. J Virol 70:2789–2796

Cohrs RJ, Randall J, Smith J, Gilden DH, Dabrowski C, van Der Keyl H, Tal-Singer R (2000) Analysis of individual human trigeminal ganglia for latent herpes simplex virus type 1 and varicella-zoster virus nucleic acids using real-time PCR. J Virol 74:11464–11471

Dingwell KS, Brunetti CR, Hendricks RL, Tang Q, Tang M, Rainbow AJ, Johnson DC (1994) Herpes simplex virus glycoproteins E and I facilitate cell-to-cell spread in vivo and across junctions of cultured cells. J Virol 68:834–845

Dingwell KS, Doering LC, Johnson DC (1995) Glycoproteins E and I facilitate neuron-to-neuron spread of herpes simplex virus. J Virol 69:7087–7098

Grinfeld E, Kennedy PG (2004) Translation of varicella-zoster virus genes during human ganglionic latency. Virus Genes 29:317–319

Hufner K, Derfuss T, Herberger S, Sunami K, Russell S, Sinicina I, Arbusow V, Strupp M, Brandt T, Theil D (2006) Latency of alpha-herpes viruses is accompanied by a chronic inflammation in human trigeminal ganglia but not in dorsal root ganglia. J Neuropathol Exp Neurol 65:1022–1030

Ito H, Sommer MH, Zerboni L, He H, Boucaud D, Hay J, Ruyechan W, Arvin AM (2003) Promoter sequences of varicella-zoster virus glycoprotein I targeted by cellular transactivating factors Sp1 and USF determine virulence in skin and T cells in SCIDhu mice in vivo. J Virol 77:489–498

Jones JO, Sommer M, Stamatis S, Arvin AM (2006) Mutational analysis of the varicella-zoster virus ORF62/63 intergenic region. J Virol 80:3116–3121

Kennedy PG, Grinfeld E, Gow JW (1998) Latent varicella-zoster virus is located predominantly in neurons in human trigeminal ganglia. Proc Natl Acad Sci USA 95:4658–4662

Kennedy PG, Grinfeld E, Gow JW (1999) Latent varicella-zoster virus in human dorsal root ganglia. Virology 258:451–454

Ku CC, Padilla JA, Grose C, Butcher EC, Arvin AM (2002) Tropism of varicella-zoster virus for human tonsillar CD4(+) T lymphocytes that express activation, memory, and skin homing markers. J Virol 76:11425–11433

Ku CC, Zerboni L, Ito H, Graham BS, Wallace M, Arvin AM (2004) Varicella-zoster virus transfer to skin by T Cells and modulation of viral replication by epidermal cell interferon-alpha. J Exp Med 200:917–925

Li Q, Ali MA, Cohen JI (2006) Insulin degrading enzyme is a cellular receptor mediating varicella-zoster virus infection and cell-to-cell spread. Cell 127:305–316

Li Q, Krogmann T, Ali MA, Tang WJ, Cohen JI (2007) The amino terminus of varicella-zoster virus (VZV) glycoprotein E is required for binding to insulin-degrading enzyme, a VZV receptor. J Virol 81:8525–8532

Lungu O, Panagiotidis CA, Annunziato PW, Gershon AA, Silverstein SJ (1998) Aberrant intracellular localization of Varicella-Zoster virus regulatory proteins during latency. Proc Natl Acad Sci USA 95:7080–7085

Mahalingam R, Wellish M, Cohrs R, Debrus S, Piette J, Rentier B, Gilden DH (1996) Expression of protein encoded by varicella-zoster virus open reading frame 63 in latently infected human ganglionic neurons. Proc Natl Acad Sci USA 93:2122–2124

Marmigere F, Ernfors P (2007) Specification and connectivity of neuronal subtypes in the sensory lineage. Nat Rev Neurosci 8:114–127

Moffat J, Mo C, Cheng JJ, Sommer M, Zerboni L, Stamatis S, Arvin AM (2004) Functions of the C-terminal domain of varicella-zoster virus glycoprotein E in viral replication in vitro and skin and T-cell tropism in vivo. J Virol 78:12406–12415

Montelius A, Marmigere F, Baudet C, Aquino JB, Enerback S, Ernfors P (2007) Emergence of the sensory nervous system as defined by Foxs1 expression. Differentiation 75:404–417

Nagel MA, Choe A, Traktinskiy I, Cordery-Cotter R, Gilden D, Cohrs RJ (2011) Varicella-zoster virus transcriptome in latently infected human ganglia. J Virol 85:2276–2287

Oliver SL, Zerboni L, Sommer M, Rajamani J, Arvin AM (2008) Development of recombinant varicella-zoster viruses expressing luciferase fusion proteins for live in vivo imaging in human skin and dorsal root ganglia xenografts. J Virol Methods 154:182–193

Pevenstein SR, Williams RK, McChesney D, Mont EK, Smialek JE, Straus SE (1999) Quantitation of latent varicella-zoster virus and herpes simplex virus genomes in human trigeminal ganglia. J Virol 73:10514–10518

Polcicova K, Goldsmith K, Rainish BL, Wisner TW, Johnson DC (2005) The extracellular domain of herpes simplex virus gE is indispensable for efficient cell-to-cell spread: evidence for gE/gI receptors. J Virol 79:11990–12001

Reichelt M, Zerboni L, Arvin AM (2008) Mechanisms of varicella-zoster virus neuropathogenesis in human dorsal root ganglia. J Virol 82:3971–3983

Saldanha CE, Lubinski J, Martin C, Nagashunmugam T, Wang L, van Der Keyl H, Tal-Singer R, Friedman HM (2000) Herpes simplex virus type 1 glycoprotein E domains involved in virus spread and disease. J Virol 74:6712–6719

Theil D, Derfuss T, Paripovic I, Herberger S, Meinl E, Schueler O, Strupp M, Arbusow V, Brandt T (2003) Latent herpesvirus infection in human trigeminal ganglia causes chronic immune response. Am J Pathol 163:2179–2184

Tirabassi RS, Enquist LW (2000) Role of the pseudorabies virus gI cytoplasmic domain in neuroinvasion, virulence, and posttranslational N-linked glycosylation. J Virol 74:3505–3516

Wang K, Lau TY, Morales M, Mont EK, Straus SE (2005) Laser-capture microdissection: refining estimates of the quantity and distribution of latent herpes simplex virus 1 and varicella-zoster virus DNA in human trigeminal ganglia at the single-cell level. J Virol 79:14079–14087

Zerboni L, Ku CC, Jones CD, Zehnder JL, Arvin AM (2005) Varicella-zoster virus infection of human dorsal root ganglia in vivo. Proc Natl Acad Sci USA 102:6490–6495

Zerboni L, Reichelt M, Jones CD, Zehnder JL, Ito H, Arvin AM (2007) From the cover: aberrant infection and persistence of varicella-zoster virus in human dorsal root ganglia in vivo in the absence of glycoprotein I. Proc Natl Acad Sci USA 104:14086–14091

Zerboni L, Reichelt M, Arvin A (2010) Varicella-zoster virus neurotropism in SCID mouse-human dorsal root ganglia xenografts. Curr Top Microbiol Immunol 342:255–276

Zerboni L, Berarducci B, Rajamani J, Jones CD, Zehnder JL, Arvin A (2011a) Varicella-zoster virus glycoprotein E is a critical determinant of virulence in the SCID mouse-human model of neuropathogenesis. J Virol 85:98–111

Zerboni L, Sobel RA, Lai M, Triglia R, Steain M, Abendroth A, Arvin A (2011b) Apparent expression of varicella-zoster virus protein in latency resulting from reactivity of murine and rabbit antibodies with human blood group A determinants in sensory neurons. J Virology (in press)

Zhu Z, Hao Y, Gershon MD, Ambron RT, Gershon AA (1996) Targeting of glycoprotein I (gE) of varicella-zoster virus to the trans-Golgi network by an AYRV sequence and an acidic amino acid-rich patch in the cytosolic domain of the molecule. J Virol 70:6563–6575